

Shock Filter: A Powerful Tool to Map Basement Blocks and Faults in the Peace River Arch of Alberta Based on Magnetic Signatures

Hassan H. Hassan*, Fugro Gravity & Magnetic Services, Inc., Calgary, Alberta, Canada
hhassan@fugro.com

and

Janine Weber, Fugro Gravity & Magnetic Services, Inc., Houston, Texas, USA

GeoConvention 2012: Vision

Summary

Spatial magnetic discontinuities displayed on aeromagnetic images often correspond to subsurface structural features such as basement blocks and their bounding faults. Their detection is of utmost importance stage in interpreting aeromagnetic maps because they have significant impact on oil and gas exploration. This abstract introduces a relatively new filtering technique to enhance these basement features known as 'shock filtering'. Shock filtering enhanced the signature made by basement blocks and their bounding faults on aeromagnetic images. This filtering technique is based on partial differential equations (PDE) and was introduced by Osher and Rudin in 1990. Shock filters create strong discontinuities at magnetic edges, and within a region of similar magnetic signature the filtered signal becomes flat. Therefore, shock filtering is able to map fault blocks within crystalline basement in a manner similar to the terracing technique developed by Cordell and McCafferty at the USGS in 1989, which transforms smoothly varying magnetic anomalies into domains of uniform properties separated by sharp boundaries that look more like a geological map.

This shock filter was applied to the reduced-to-pole regional total aeromagnetic intensity grid covering the Peace River Arch of the Western Canada Sedimentary Basin. The total intensity grid was derived from the public domain aeromagnetic database provided by the Geological Survey of Canada. The results obtained from applying shock filters on the aeromagnetic image are very interesting: in addition to mapping structural discontinuities that might be associated with basement faults, the shock filter was able to segment magnetic anomalies into zones of uniform properties with different magnetic signatures. These segments are most likely related to different fault blocks or geological domains in the basement. This abstract discusses how basement blocks and block faults in the Precambrian basement of the Peace River Arch were mapped using shock filters.

Introduction

In this study a robust filtering technique known as 'shock filtering' was applied to the publicly available regional aeromagnetic grid covering part of the prominent Peace River Arch (PRA) structure of the Western Canada Sedimentary Basin (Figs. 1 and 2). The regional total magnetic intensity aeromagnetic grid used for this purpose was assembled from various aeromagnetic surveys that were acquired over the period from 1990 to 1992, mainly by GSC. The main purpose of this study was to test the ability of shock filters to enhance the detection of blocks and faults in the Precambrian crystalline basement of the PRA structure. The PRA is a large E-NE trending anticlinal structure in the Western Canada Sedimentary Basin. It extends from northeast British Columbia into northwest Alberta for approximately 750 km (O'Connell, 1994). The overlying Middle Devonian to Upper Cretaceous sedimentary rocks have been a focus of extensive oil and gas exploration since 1949. Although most of the research in the PRA area has focused on exploration of the overlying sedimentary strata, some of the mechanisms

created the oil and gas traps have been found to be fault controlled. The Precambrian core of the PRA consists mainly of granites that have been subjected to several tectonic episodes over the past 400 million years. Each tectonic episode created its own set of fractures and faults that eventually acted as structural traps for oil and gas accumulation. The main structural elements of the study area are displayed in Figure 2.



Figure 1. Location of the study area

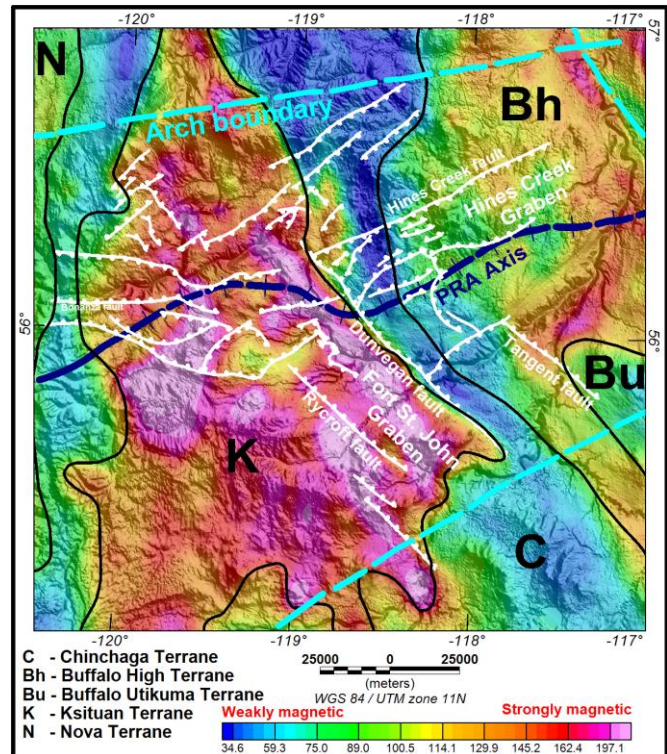


Figure 2. Major structural elements of Peace River Arch overlain on the total magnetic intensity grid. Thrust faults in white, teeth on the upthrown side.

Theory and Methodology

Shock filters were introduced by Osher and Rudin in 1990; they are a type of hyperbolic partial differential equation. Most of the research involving the application of partial differential equations in image processing focused on parabolic equations. Shock filters create strong discontinuities at geological edges, and within a region, the filtered signal becomes flat. Therefore, shock filters are ideal for mapping basement blocks and their bounding basement faults on the basis of their magnetic signatures. Locating basement faults and fractures is very important as they provide the flow paths necessary for oil and gas accumulation. Examples of shock filter response to a step-edge and to a sine wave signal without noise are shown in Figures 3 and 4, respectively.

The formula for shock filters as described by Gilboa *et al.* (2002) is as follows:

$$\frac{\partial I}{\partial t} = |I_x| F(I_{xx})$$

where I represents the image and I_x and I_{xx} represent the first and the second directional derivatives of the image I , respectively.

F should satisfy $F(0) = 0$, $F(s)\text{sign}(s) \geq 0$.

Choosing $F(s) = \text{sign}(s)$ yields the classical shock filter equation:

$$\frac{\partial I}{\partial t} = -\text{sign}(I_{xx})|I_x|$$

Because of the second derivative term in the formula, shock filters are sensitive to noise. Therefore, in order to increase robustness of shock filters it is important to convolve the image's second derivative with a low-pass filter, such as a Gaussian:

$$\frac{\partial I}{\partial t} = -\text{sign}(G_\sigma * I_{xx})|I_x|$$

where σ is the standard deviation of Gaussian function.

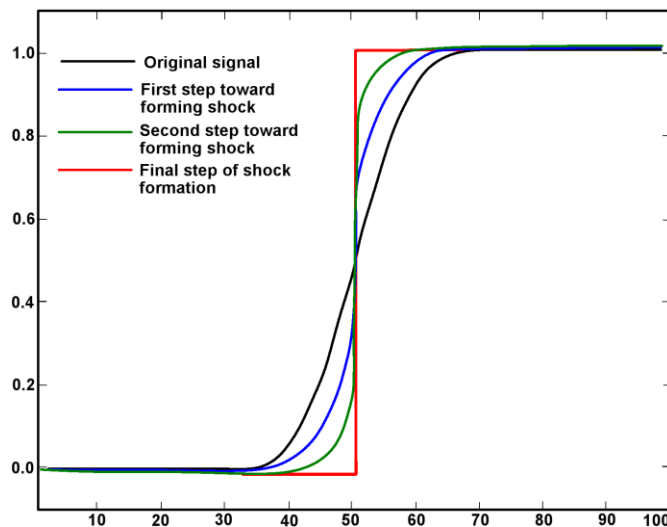


Figure 3. Shock filter response to step-edge steady state shock filter solution

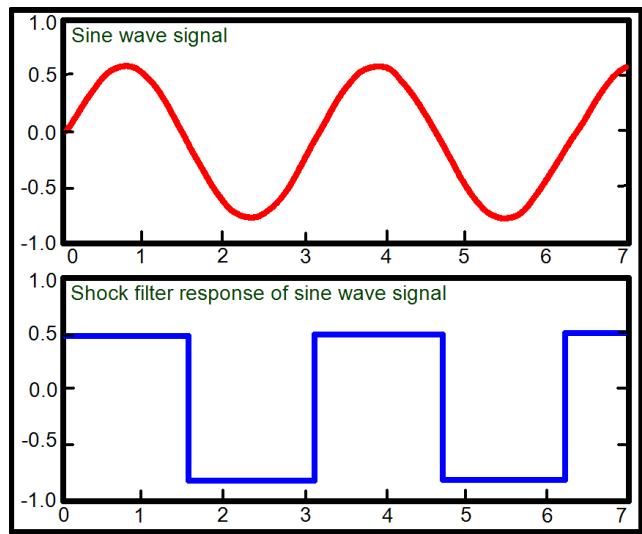


Figure 4. Shock filter response to sine wave signal

Examples

Shock filtering was applied to the RTP image (Fig. 2) of the study area. Prior to applying the filter it was convolved with a Gaussian filter using a standard deviation of 3.0 to reduce the level of noise. The output image after applying the shock filter is shown in Figures 5 and 6. The images clearly show that the shock filter flattened areas with similar magnetic signatures (Fig. 5) and at the same time enhanced the response of faults (Fig. 6) at the border of basement blocks. It is also interesting to note that some of the faults (but not all) in the area that were previously mapped using seismic appear to coincide with faults identified by the shock filter. The seismic-mapped faults are primarily in the supra-basement rocks while the magnetically-defines structures are primarily within the basement. Thus, the faults that coincide with the shock filtered display may be deep-seated, while the non-coincident structures may be solely within the sedimentary section.

Conclusions

Shock filters applied to regional aeromagnetic data over part of the PRA area appear to provide a powerful tool for mapping basement blocks on the basis of their magnetic signature. In addition to mapping basement blocks as flat surfaces with similar magnetic properties, faults and lithological contacts bounding these blocks were also significantly enhanced. The results also show that in many cases it appears that some of the structures mapped by shock filtering correlate to some degree with faults mapped by seismic method.

References

Cordell, Lindriith, and McCafferty, A.E., 1989, A terracing operator for physical property mapping with potential field data: *Geophysics*, **54**, 621-634.

Gilboa, G., Sochen, N., and Zeevi, Y. Y., 2002, Regularized shock filters and complex Diffusion: ECCV-'02, LNCS 2350, pp. 399-313, Springer-Verlag.

O'Connell, S.C., 1994, Geological history of the Peace River Arch; in *Geological Atlas of the Western Canada Sedimentary Basin*, G.D. Mossop and I. Shetsen (comp.), Canadian Society of Petroleum Geologists and Alberta Research Council, Special Report **4**, 431-438.

Osher, S., and Rudin, L., 1990, Feature-oriented image enhancement using shock filters: *SIAM Journal of Numerical Analysis*, **27**, 919-949.

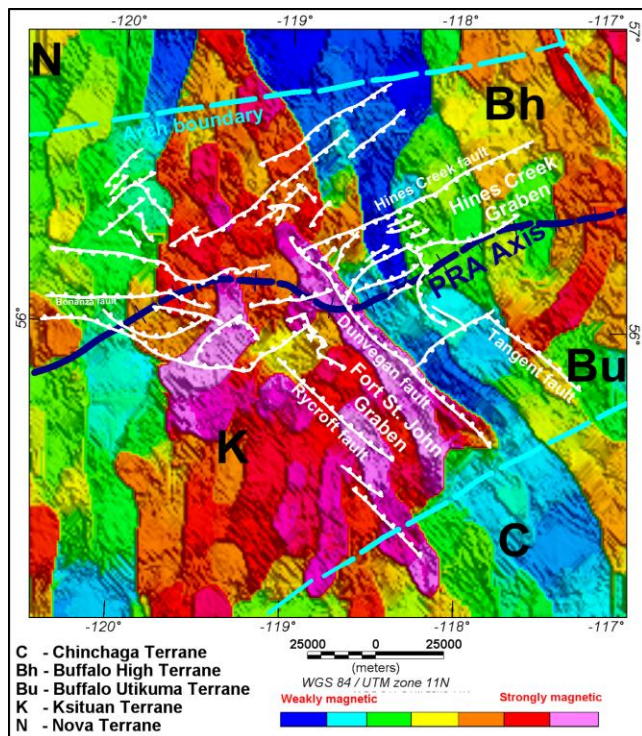


Figure 5. Shock filter of TMI showing different basement blocks

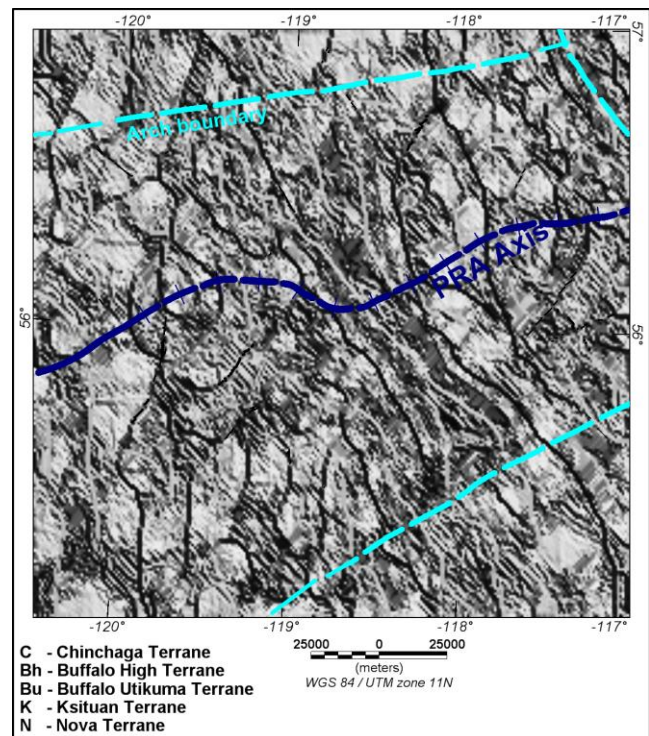


Figure 6. Shock filter of TMI showing basement faults